

A hybrid tau-leap for simulating chemical kinetics with applications to parameter estimation

Thomas Trigo Trindade and Konstantinos C. Zygalakis

August 2023

Abstract

We consider the problem of efficiently simulating stochastic models of chemical kinetics. The Gillespie Stochastic Simulation algorithm (SSA) is often used to simulate these models, however, in many scenarios of interest, the computational cost quickly becomes prohibitive. This is further exasperated in the Bayesian inference context when estimating parameters of chemical models, as the intractability of the likelihood requires multiple simulations of the underlying system. To deal with issues of computational complexity in this paper, we propose a novel hybrid τ -leap algorithm for simulating well-mixed chemical systems. In particular, the algorithm uses τ -leap when appropriate (high population densities), and SSA when necessary (low population densities, when discrete effects become non-negligible). In the intermediate regime, a combination of the two methods, which leverages the properties of the underlying Poisson formulation, is employed. As illustrated through a number of numerical experiments the hybrid τ offers significant computational savings when compared to SSA without however sacrificing the overall accuracy. This feature is particularly welcomed in the Bayesian inference context, as it allows for parameter estimation of stochastic chemical kinetics at reduced computational cost.

1 Introduction

In the last few years, there has been an increase in the interest in biochemical systems with a small number of interacting components, see for example the phage λ -lysis decision circuit [1], circadian rhythms [2] as well as the cell cycle [3]. In the setting of low copy numbers of interacting components, the stochastic variations may constitute a crucial element in the description of the dynamics of the systems, often in the form of bursts and cascading mechanisms that are typically not well captured by macroscopic models. Additionally, the general consensus now is that accounting for the stochasticity plays a central role in the interpretation of experimental data originating from cell and molecular processes [4, 5].

Even when incorporating stochasticity in the modelling of biochemical systems one needs to decide on the assumptions that hold for the system in question. In particular, when the underlying system is not well-mixed the appropriate microscopic description involves describing the dynamics of each particle dynamics separately [6, 7]. On the other hand, when the system is sufficiently well mixed the kinetics of each species are described by a continuous time discrete space Markov chain, and in this case, the corresponding master equation is known as the Chemical Master Equation (CME) [8]. Essentially, the CME is a (potentially infinite-dimensional) system of Ordinary Differential Equations (ODEs) that describes, at each point in time, the probability density of all the different possible states of the system.

Except for some very simple chemical systems [9], due to the inherent high dimensionality of the CME, analytic solutions of the CME are not available. Therefore several methods have been developed [10, 11, 12] that try to solve the corresponding system of differential equations directly. An alternative and more widely adopted approach relates to the direct simulation of the underlying Markov process. More precisely, the stochastic simulation algorithm (SSA) [13] exactly simulates trajectories whose probability density function matches that of the CME as the system evolves in time. In addition, several alternative exact algorithms have been subsequently proposed [14, 15] that were shown to be computationally more efficient than SSA. The core idea behind these algorithms is that one samples a waiting time for the next reaction from an appropriate exponential distribution, while another draw of a random variable is then used to decide which of the possible reactions will occur.

A fundamental issue with all the exact algorithms described above is that running them can be computationally intensive for realistic problems. The reason behind this is that the time between subsequent reactions becomes very small leading thus to a computational bottleneck. This issue is further exasperated when one is interested in estimating parameters of the stochastic kinetics models from data, since the underlying likelihood is intractable, and one needs to perform multiple stochastic simulations to deal with this intractability [16, 17].

One approach to deal with the computational complexity of exact algorithms like SSA, is to use an approximate algorithm such as τ -leap [18] in which the system is simulated over suitable time intervals for which several chemical events might occur. This lumping of chemical events can lead to significant computational savings [8]. Furthermore, several variants of this algorithm have been proposed in the literature [19, 20, 21, 22]. An alternative approach to speeding up the SSA is to employ different approximations on the level of the description of the chemical system. A prime example of this is the reaction rate [8] equation (RRE). This is an ODE that is valid in the limit of large molecular populations, and it can be thought of as approximating the time evolution of the mean of the evolving Markov chain. An intermediate regime between the SSA and the reaction rate equation is the one where stochasticity is still important, but there exists a sufficient number of molecules to describe the evolving kinetics by a continuous model. This regime is called the chemical Langevin equation (CLE) [23], which is an Itô stochastic differential equation (SDE) driven by a

multidimensional Wiener process.

In practice, a lot of chemical systems can contain many different species with a wide range of population numbers. This multi-scale nature makes the direct application of approximate methods such as τ -leap or of approximate models such as the CLE or the RRE non-trivial. This has motivated several different hybrid algorithms [24, 25, 26] that only treat certain chemical species as continuous variables and others as discrete. By doing so, such schemes can benefit from the computational efficiency of continuum approximations (either deterministic or stochastic) while still taking into account discrete fluctuations when necessary. Such schemes typically involve partitioning the reactions into *fast* and *slow* reactions, with the fast reactions modeled using a continuum approximation (CLE or the reaction rate equation), while using the Markov jump process to simulate the discrete reactions. Chemical species that are affected by fast reactions are then modeled as continuous variables while the others are kept discrete. Since the reaction rate depends on the state, some fast reactions may become slow and vice versa. This issue can be addressed by periodic re-partitioning [27, 28]. A recent approach that doesn't require explicit knowledge of which reactions are fast and which slow was proposed in [29]. In particular, the algorithm would perform Langevin dynamics in regions of abundance, jump dynamics in regions where one of the involved chemical species is in small concentrations, and a mixture of both in intermediate regions

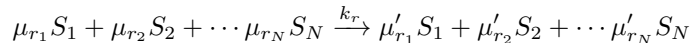
In this paper inspired by the work in [29] we propose a hybrid τ -leap scheme that uses τ -leaping dynamics to simulate reactions in which the discreteness cannot be discounted. Furthermore, our scheme does not explicitly keep track of fast and slow reactions, but rather, performs τ -leap dynamics in regions of abundance, jump dynamics in regions where one of the involved chemical species is in small concentrations, and a mixture of both in intermediate regions. The preference of jump over τ -leap dynamics is controlled for each individual reaction using a blending function which is chosen to take value 1 in regions of low concentration, 0 in regions where all involved chemical species are abundant, and smoothly interpolates in between. The choice of each blending region will depend on the reaction rate associated with the given reaction. The region should be generally chosen so that the resulting propensity is large in the τ -leaping region and small in the discrete region.

The rest of the paper is organized as follows. In Section 2, we review the standard approaches for simulating chemical kinetics such as SSA and the τ -leap method as well as reviewing the main ideas behind the CLE. Furthermore, we introduce some basic ideas associated with parameter estimation for chemical kinetics, highlighting the fact that since the underlying likelihood is intractable one needs to design inference algorithms based on using fast and accurate simulations of the underlying chemical system. Then, in Section 3, we introduce our new hybrid τ algorithm, while in Section 4 we perform a number of numerical simulations that demonstrate the excellent performance of the proposed numerical scheme when compared to other state-of-the-art methods. We conclude in Section 5 with a summary of our findings and a discussion of future directions.

2 Preliminaries

We will consider a biochemical network of N species that interact through M reaction channels within an isothermal reactor of fixed volume V . We will denote with $X_i(t), i = 1, \dots, N$ the number of molecules of species S_i at time t and let $\mathbf{X}(t) = (X_1(t), \dots, X_N(t))$. Throughout this work, we will assume that the chemical species are well mixed and hence $\mathbf{X}(t)$ can be modeled as a continuous time discrete space Markov process [30]. More precisely, when in state $\mathbf{X}(t)$, the j -th reaction gives rise to a transition $\mathbf{X}(t) \rightarrow \mathbf{X}(t) + \boldsymbol{\nu}_j$ with exponential distributed waiting time with inhomogeneous rate $a_j(\mathbf{X}(t))$ where $a_j(\cdot)$ and $\boldsymbol{\nu}_j \in \mathbb{Z}^N$ denote the propensity and stoichiometric vector corresponding to the j -th reaction, respectively.

Each reaction is of the form



where $r = 1, \dots, M$ and $\mu_{r_i}, \mu'_{r_i} \in \mathbb{N} = \{0, 1, 2, \dots\}$, for $i = 1, \dots, N$. We will denote with $\boldsymbol{\mu} = (\mu_{r_1}, \dots, \mu_{r_N})$, $\boldsymbol{\mu}' = (\mu'_{r_1}, \dots, \mu'_{r_N})$ and then we have that the stoichiometric vectors $\boldsymbol{\nu}_r, r = 1, \dots, M$ satisfy

$$\boldsymbol{\nu}_r = \boldsymbol{\mu}'_r - \boldsymbol{\mu}_r.$$

These vectors describe how much the number of molecules change when the r -th reaction takes place. For notational convenience, hereafter, $V = [\boldsymbol{\nu}_1, \dots, \boldsymbol{\nu}_M]$. Under the assumptions of mass action kinetics, the associated propensity a_r for the r -th reaction is

$$a_r(\mathbf{x}) = c_r \prod_{j=1}^N \frac{x_j!}{(x_j - \mu_{r_j})!}$$

where x_j is the number of molecules of S_j . Again, for notational convenience, hereafter $\mathbf{a}(\mathbf{x}) = (a_1(\mathbf{x}), \dots, a_M(\mathbf{x}))$.

2.1 Algorithms for simulating chemical kinetics

The main assumption in modelling the evolution of $\mathbf{X}(t)$ is that within the time interval $[t, t + dt)$, the probability of the reaction j firing is proportional to $a_j(\mathbf{X}(t))dt + o(dt)$. The process $\mathbf{X}(t)$ can thus be expressed as the sum of M Poisson processes with inhomogeneous rates $a_j(\mathbf{X}(t))$. Furthermore, the process $\mathbf{X}(t)$ can be expressed [23, 31] as a random time change of unit rate Poisson processes

$$\mathbf{X}(t) = \mathbf{X}(0) + \sum_{r=1}^M P_r \left(\int_0^t a_r(\mathbf{X}(s)) ds \right) \boldsymbol{\nu}_r \quad (1)$$

where P_r are independent unit-rate Poisson processes. This formulation of the stochastic process is very helpful in terms of designing numerical methods that

Algorithm 2.1: Stochastic Simulation Algorithm (SSA)

Input : $T > 0$, stoich. matrix V , propensities $\mathbf{a}(\mathbf{x})$ **Output:** Exact realisation of $\{\mathbf{X}_t\}_{t \in [0, T]}$ 1 $t = 0$;2 **while** $t < T$ **do**3 Let $a_0 = \sum_{j=1}^M a_j(\mathbf{X}(t))$;4 Sample $\tau \sim -\log u/a_0$, where $u \sim \mathcal{U}[0, 1]$;5 Choose the next reaction r with probability $a_r(\mathbf{X}(t))/a_0$, where $r = 1, \dots, M$;6 $\mathbf{X}(t + \tau) = \mathbf{X}(t) + \boldsymbol{\nu}_r$;7 $t = t + \tau$.

produce either exact or approximate samples. In particular, the standard way of sampling realisations of $\mathbf{X}(t)$ is the Gillespie SSA [32] see Algorithm 2.1.

As we can see in Algorithm 2.1 in order to advance the system from time t to time $t + \tau$ one needs to generate two random variables. The next reaction method [33] exploits further the structure of (1) to provide a more efficient implementation of Gillespie's SSA when simulating systems with many reaction channels. However, a fundamental computational issue with exact algorithms such as Gillespie's SSA or the next reaction method is they become computationally expensive when the number of molecules becomes large. In particular, in this case, the time to the next reaction becomes small, and if one is interested in simulating the chemical systems to time scales of $\mathcal{O}(1)$ will have to simulate a very high number of reaction events.

One approach for speeding up exact algorithms is to further exploit the structure of (1) to construct approximate algorithms. In particular, instead of explicitly calculating the time to the next reaction, one can choose a timescale of interest τ and then calculate how many reactions have occurred in each of the reaction channels. More precisely, one can use the following approximation

$$\int_t^{t+\tau} a_j(\mathbf{X}(s)) ds \simeq a_j(\mathbf{X}(t))\tau$$

and then using the formulation (1) is not difficult to see that the number of reactions k_j in the j -th channel can be approximated by

$$k_j \sim \mathcal{P}(\alpha_j(\mathbf{X}(t))\tau)$$

The corresponding algorithm is called τ -leaping, see also Algorithm 2.2. The main computational savings here come from the fact that several reaction events are lumped together, while in addition under appropriate assumptions on the propensity functions of the system [34, 35] the error induced by this approximation is not very large. However, unlike exact methods like SSA in principle, the simple τ -leap method might lead to negative populations, so one has to modify the original algorithm to avoid this issue [20, 36].

Algorithm 2.2: τ -leap

Input : $T > 0$, stoich. matrix V , propensities $\mathbf{a}(\mathbf{x})$, $\tau > 0$

Output: Approximate realisation of $\{\mathbf{X}_t\}_{t \in [0, T]}$

```
1  $t \leftarrow 0$ ;  
2 while  $t < T$  do  
3   for  $j = 1, \dots, M$  do  
4      $k_j \sim \mathcal{P}(a_j(\mathbf{X}(t))\tau)$  ;  
5      $\mathbf{X}(t + \tau) = \mathbf{X}(t) + \sum_{j=1}^M \boldsymbol{\nu}_j k_j$ ;  
6      $t = t + \tau$ 
```

2.1.1 Diffusion approximation

One can further exploit the structure of (1) to construct a Markov process $\mathbf{Y}(t)$ to approximate $\mathbf{X}(t)$. The difference is now that instead of taking values on \mathbb{N}^N like $\mathbf{X}(t)$, $\mathbf{Y}(t)$ takes values in \mathbb{R}^N . More precisely, $\mathbf{Y}(t)$ is the solution to the following SDE

$$d\mathbf{Y}(t) = \sum_{j=1}^M \boldsymbol{\nu}_j a_j(\mathbf{Y}(t)) dt + \sum_{j=1}^M \boldsymbol{\nu}_j \sqrt{a_j(\mathbf{Y}(t))} dW_j(t). \quad (2)$$

which is known as the chemical Langevin equation (CLE). It is possible to show that under specific assumptions [37, 23, 31] $\mathbf{Y}(t)$ is indeed a very good approximation to $\mathbf{X}(t)$. Furthermore, since (2) is an SDE, analytic solutions to

Algorithm 2.3: CLE Euler-Maruyama (CLE-EM)

Input : $T > 0$, stoich. matrix V , propensities $\mathbf{a}(\mathbf{x})$, $\tau > 0$

Output: EM approximation of (2)

```
1  $t \leftarrow 0$ ;  
2 while  $t < T$  do  
3   for  $j = 1, \dots, M$  do  
4      $\xi_j \stackrel{i.i.d.}{\sim} \mathcal{N}(0, 1)$   
5      $\mathbf{Y}(t + \tau) = \mathbf{Y}(t) + \tau \sum_{j=1}^M \boldsymbol{\nu}_j a_j(\mathbf{Y}(t)) + \sqrt{\tau} \sum_{j=1}^M \boldsymbol{\nu}_j \sqrt{a_j(\mathbf{Y}(t))} \xi_j$  ;  
6      $t = t + \tau$ 
```

it are not available except for some very simple models. One thus has to resort to numerical simulations and Algorithm 2.3 describes a simple discretization of (2) based on the Euler-Maruyama method.

Similarly to the case of τ -leap, one has to be careful in how they choose the time-step τ since Algorithm 2.3 might lead to negative populations. However, unlike τ -leap where this could be addressed by taking τ -smaller and essentially simulating closer the dynamics of (1), the negativity issue can persist even

in the limit of small τ since there is no guarantee that the solutions to the CLE equation will remain non-negative [8]. Many different alternatives have been proposed to address the issue of non-negativity ranging from considering a complex-valued CLE [38], an appropriately constrained CLE [39], or a model that seamlessly interpolates between the fully discrete formulation (1) and the CLE (2) [29].

2.2 Parameter estimation for chemical kinetics

In many practical applications one might be interested in estimating parameters of stochastic kinetics models such as reaction rates from time series data. In the typical setting [40, 41] given a realisation of the stochastic process $\{\mathbf{X}_t, t \in [0, T]\} =: \mathbf{X}_{[0, T]}$, the law of which depends on some parameter \mathbf{c} , we consider the problem of inferring the value of \mathbf{c} while having access only to discrete and noisy observations \mathbf{y}_{I_N} of $\mathbf{X}_{[0, T]}$ at times $I_N = (i_1, \dots, i_N) \subset [0, T]$.

In our setting, the true data $\mathbf{x}_{[0, T]}$ is a realisation of a stochastic chemical system $\mathbf{X}_{[0, T]}$. That true data is (for simplicity) measured and saved at integer times $\llbracket 0, T \rrbracket := \{0, 1, \dots, T\}$, during which measurement errors are possible. This leads to the noisy data $\mathbf{y}_{[0, T]}$ (a realisation of $\mathbf{Y}_{[0, T]}$). The observations $\mathbf{Y}_{[0, T]}$ are assumed to be conditionally independent given $\mathbf{X}_{[0, T]}$.

We aim to characterise or sample from the probability density $\mathbb{P}(\mathbf{c} | \mathbf{y}_{[0, T]})$, to which end we use a Markov chain targetting that density. By Bayes' theorem,

$$\mathbb{P}(\mathbf{c} | \mathbf{y}_{[0, T]}) = \frac{\mathbb{P}(\mathbf{y}_{[0, T]} | \mathbf{c}) \mathbb{P}_0(\mathbf{c})}{\mathbb{P}(\mathbf{y}_{[0, T]})} \quad (3)$$

Here, $\mathbb{P}_0(\mathbf{c})$ is a prior of the parameter distribution. Using the law of total probability on the denominator, we obtain

$$\mathbb{P}(\mathbf{c} | \mathbf{y}_{[0, T]}) \propto \mathbb{P}_0(\mathbf{c}) \int \mathbb{P}(\mathbf{y}_{[0, T]} | \mathbf{x}_{[0, T]}, \mathbf{c}) \mathbb{P}(\mathbf{x}_{[0, T]} | \mathbf{c}) d\mathbf{x}_{[0, T]}. \quad (4)$$

As the following example reveals, the likelihood (4) is intractable, even in the case where there is no noise in the data $\mathbf{y}_{[0, T]}$ and one observes $\mathbf{x}_{[0, T]}$ directly.

Example 2.1 *We consider the simplest case where the data $\mathbf{y}_{[0, T]}$ coincide exactly with $\mathbf{x}_{[0, T]}$. In this case, $\mathbb{P}(\mathbf{y}_{[0, T]} | \mathbf{c})$ becomes*

$$\mathbb{P}(\mathbf{y}_{[0, T]} | \mathbf{c}) = \prod_{i=1}^T p(\mathbf{Y}(t_i) | \mathbf{c}, \mathbf{Y}(t_{i-1})),$$

where $p(\mathbf{Y}(t_i) | \mathbf{c}, \mathbf{Y}(t_{i-1}))$ is the solution to the CME. However, except for some very simple chemical systems [9], solutions to the CME are not analytically available which in turn implies that the likelihood $\mathbb{P}(\mathbf{y}_{[0, T]} | \mathbf{c})$ is in general intractable.

As the Example 2.1 indicates the likelihood $\mathbb{P}(\mathbf{y}_{[0, T]} | \mathbf{c})$ is intractable. There are different ways of dealing with this issue, one of which is through approximate

Bayesian computation [17]. However, here we choose to proceed by following the pseudo-marginal approach [42], similarly to what was done in [16]. In particular, the idea is that if we have access to an unbiased estimator $\hat{\mathbb{P}}(\mathbf{y}_{[0,T]} | \mathbf{c})$ of our intractable likelihood $\mathbb{P}(\mathbf{y}_{[0,T]} | \mathbf{c})$ we can proceed in the standard manner to perform Bayesian inference within a Metropolis-Hastings framework by replacing the intractable likelihood by its unbiased estimator.

2.2.1 Particle Pseudo-Marginal Metropolis–Hastings algorithm

As discussed above within the pseudo-marginal framework we need to have access to an unbiased estimator of our intractable likelihood. We do this by using a (bootstrap) particle filter [43] with importance resampling to iteratively construct the (unbiased) estimate of $\mathbb{P}(\mathbf{c} | \mathbf{y}_{[0,T]})$. Combing this unbiased estimate with a Metropolis-Hastings step gives rise to the Particle Pseudo-Marginal Metropolis–Hastings algorithm (PPMMH) [41], see Algorithm 2.4. In typical Metropolis-Hastings fashion, the state space is explored via a proposal kernel $q(\cdot | \mathbf{c})$ generating proposals \mathbf{c}^* from the current state \mathbf{c} , and the proposals are kept in the chain using a Metropolis-Hastings accept/reject mechanism.

Algorithm 2.4: Particle Pseudo-Marginal Metropolis–Hastings

Output: Samples $\mathbf{c}_i \sim \mathbb{P}(\cdot | \mathbf{y}_{[0,T]})$

- 1 **for** $i = 1, \dots$ **do**
- 2 generate proposal $\mathbf{c}^* \sim q(\cdot | \mathbf{c})$;
- 3 compute $\hat{\mathbb{P}}(\mathbf{y}_{[0,T]} | \mathbf{c}^*)$;
- 4 accept \mathbf{c}^* with probability

$$\min \left\{ \frac{\hat{\mathbb{P}}(\mathbf{y}_{[0,T]} | \mathbf{c}^*) \mathbb{P}_0(\mathbf{c}^*)}{\hat{\mathbb{P}}(\mathbf{y}_{[0,T]} | \mathbf{c}^{(i-1)}) \mathbb{P}_0(\mathbf{c}^{(i-1)})} \times \frac{q(\mathbf{c}^{(i-1)} | \mathbf{c}^*)}{q(\mathbf{c}^* | \mathbf{c}^{(i-1)})}, 1 \right\}.$$

The bootstrap particle filter (computed in line 2 of Algorithm 2.4) relies on the fact that, for $j > 0$,

$$\mathbb{P}(\mathbf{x}_{[0,j+1]} | \mathbf{y}_{[0,j+1]}) \propto \mathbb{P}(\mathbf{y}_{j+1} | \mathbf{x}_{j+1}) \mathbb{P}(\mathbf{x}_{[0,j]} | \mathbf{y}_{[0,j]}) \mathbb{P}(\mathbf{x}_{(j,j+1)} | \mathbf{x}_{[0,j]}). \quad (5)$$

This allows refining the naive approach of simply simulating N particles/realisations up to time T . The iterative method consists in propagating the particles over a length 1 time interval, evaluating the likelihood of each particle given the data, and using an importance resampling mechanism. Among others, this allows to avoid the degeneracy of the filter [44]. The unbiasedness of the estimator can be established using, e.g., [41, p. 290]. The steps are summarised in Algorithm 2.5.

Line 7 of Algorithm 2.5 entails the repeated simulation of N particles over a time interval, resulting in a computationally intensive process. In this work, we speed up those computations by using the Hybrid- τ algorithm.

Algorithm 2.5: Bootstrap Particle Filter with Importance Resampling

Input : Proposal \mathbf{c}^*
Output: $\hat{\mathbb{P}}(\mathbf{y}_{[0,T]} | \mathbf{c}^*)$

```
1 for  $k = 1, \dots, N$  ; // Initialisation
2 do
3   draw  $\mathbf{x}_0^k \sim \mathbb{P}_0(\mathbf{x}_0)$  (prior)
4 for  $j = 0, 1, \dots, T - 1$  do
5   for  $k = 1, \dots, N$  ; // Particles
6   do
7     simulate  $\mathbf{x}_{[j,j+1]}^k \sim \mathbb{P}(\cdot | \mathbf{x}_j^k, \mathbf{c}^*)$  ;
8      $(\mathbf{x}_{[0,j+1]}^k, \tilde{\mathbf{x}}_{j+1}^k) \leftarrow (\mathbf{x}_{[0,j]}^k, \mathbf{x}_{[j,j+1]}^k)$  ;
9      $w_{jk} = \mathbb{P}(\mathbf{y}_{j+1} | \tilde{\mathbf{x}}_{j+1}^k)$  ;
10  for  $k = 1, \dots, N$  ; // Resampling
11  do
12  | sample  $\mathbf{x}_{j+1}^k$  from  $\{\tilde{\mathbf{x}}_{j+1}^\ell\}_{\ell=1}^N$  with resp. probability  $\frac{w_{j\ell}}{\sum_{s=1}^N w_{js}}$ .
13  $\hat{\mathbb{P}}(\mathbf{y}_{[0,T]} | \mathbf{c}^*) \leftarrow \hat{\mathbb{P}}(\mathbf{y}_0) \prod_{j=1}^T \left( \frac{1}{N} \sum_{k=1}^N w_{jk} \right)$ .
```

3 Hybrid τ -leap

We now introduce our proposed algorithm. The idea here is similar to the one in [29]. In particular, we will introduce one *blending* function for each reaction denoted by $\beta_j(\mathbf{x}) : \mathbb{R}^N \mapsto [0, 1]$, $j = 1, \dots, M$. One can then simply rewrite equation (1) in the following way

$$\mathbf{X}(t) = \mathbf{X}(0) + \sum_{r=1}^M P_r \left(\int_0^t \beta_r(\mathbf{X}(s)) a_r(\mathbf{X}(s)) ds + \int_0^t (1 - \beta_r(\mathbf{X}(s))) a_r(\mathbf{X}(s)) ds \right) \boldsymbol{\nu}_r$$

Using the property of Poisson processes it is now possible to rewrite the equation above in the following matter

$$\begin{aligned} \mathbf{X}(t) &= \sum_{r=1}^M P_r \left(\int_0^t \beta_r(\mathbf{X}(s)) a_r(\mathbf{X}(s)) ds \right) \boldsymbol{\nu}_r \\ &+ \sum_{r=1}^M P_r \left(\int_0^t (1 - \beta_r(\mathbf{X}(s))) a_r(\mathbf{X}(s)) ds \right) \boldsymbol{\nu}_r \end{aligned} \quad (6)$$

This rewriting might appear trivial at first sight, but it is essential in terms of explaining our algorithm given the form of the blending functions β_r . In particular, for a single-species system, a natural choice of blending function is

the following piecewise linear function

$$\beta(x, I_1, I_2) = \begin{cases} 1, & \text{if } x \leq I_1 \\ \frac{I_2 - x}{I_2 - I_1}, & \text{if } I_1 \leq x \leq I_2 \\ 0, & \text{if } x \geq I_2 \end{cases}.$$

Furthermore, in the case of a chemical system with N species, we can construct blending functions in the following way. Let R_r be the set of chemical species involved in the r -th reaction (both as reactants and products of reaction). Then we can define $\beta_r(\mathbf{x})$, $r = 1, \dots, M$ as follows

$$\beta_r(\mathbf{x}) = 1 - \prod_{n \in R_r} (1 - \beta(x_n, I_1^n, I_2^n)), \quad (7)$$

where $I_n^1 < I_n^2$, are the boundaries for each individual chemical species.

We now define the following sets

$$C_{\text{SSA}}^r = \{\mathbf{x} \in \mathbb{N}^N \mid n \in R_r, x_n \leq I_1^n\} \quad (8a)$$

$$C_{\tau\text{-leap}}^r = \{\mathbf{x} \in \mathbb{N}^N \mid n \in R_r, x_n \geq I_2^n\} \quad (8b)$$

$$C_{\text{mix}}^r = \{\mathbf{x} \in \mathbb{N}^N \mid n \in R_r, I_1^n \leq x_n \leq I_2^n\}. \quad (8c)$$

It is not difficult to see that $\mathbf{x} \in \cap_{r=1}^M C_{\text{SSA}}^r$ translates to $\min \beta_j(\mathbf{x}) = 1$, while $\mathbf{x} \in \cap_{r=1}^M C_{\tau\text{-leap}}^r$ corresponds when $\max \beta_j(\mathbf{x}) = 0$. Hence combining (7) with (6) when $\mathbf{x} \in \cap_{r=1}^M C_{\text{SSA}}^r$, we will use SSA to simulate (6), while when $\mathbf{x} \in \cap_{r=1}^M C_{\tau\text{-leap}}^r$ we will use the τ -leap to simulate (6). It is only in the region $\mathbf{x} \in \cup_{r=1}^M C_{\text{mix}}^r$ that some blending functions obtain values in $(0, 1)$ and thus we will use a combination of SSA for the term $P_r \left(\int_0^t \beta_r(\mathbf{X}(s)) a_r(\mathbf{X}(s)) ds \right)$, and τ -leap for the term $P_r \left(\int_0^t (1 - \beta_r(\mathbf{X}(s))) a_r(\mathbf{X}(s)) ds \right)$. We will call the resulting algorithm the hybrid τ -method (see Algorithm 3.1).

Example 3.1 We consider here the following chemical system



Figures 1(a)-(c) illustrate the sets $C_{\text{SSA}}^r, C_{\tau\text{-leap}}^r, C_{\text{mix}}^r$ associated with each of the reactions, here $r = 1, \dots, 4$. In addition, in Figure 1(d) we can see the partition of the state space in terms of which simulation regime is applied where.

Remark 3.2 In Algorithm 3.1 two different time-stepping strategies are being used. There is δt that relates to the time-step used by the τ -leap method in the intermediate regime and Δt that relates to the time-step used by the τ -leap method when only τ -leap is used for simulation. This is done to provide extra flexibility but is not crucial for the performance of the algorithm.

Algorithm 3.1: Hybrid- τ

Input : $T > 0$, stoich. matrix V , propensities $\mathbf{a}(\mathbf{x})$, blending functions $\{\beta_i\}_{i=1}^M$, $\delta t, \Delta t$

Output: Approximate realisation of $\{\mathbf{X}_t\}_{t \in [0, T]}$

```
1  $t \leftarrow 0$ ;  
2 while  $t < T$  do  
3   if  $\max \beta_j(\mathbf{x}) = 0$  then  
4     Perform  $\tau$ -leaping up to time  $t + \Delta t$  (with propensities  $\mathbf{a}(\mathbf{x})$ ) ;  
5      $t = t + \Delta t$  ;  
6   else if  $\min \beta_j(\mathbf{x}) = 1$  then  
7      $a_0 = \sum_{j=1}^M a_j(\mathbf{x})$  ;  
8      $\tau = -\log(\xi_1)/a_0$ , where  $\xi_1 \sim \mathcal{U}(0, 1)$  ;  
9     Choose reaction  $j$  with probability  $a_j(\mathbf{x})/a_0$  ;  
10  else  
11     $a_0 = \sum_{j=1}^M \beta_j(\mathbf{x})a_j(\mathbf{x})$  ;  
12     $\tau = -\log(\xi_1)/a_0$ , where  $\xi_1 \sim \mathcal{U}(0, 1)$  ;  
13    Choose reaction  $j$  with probability  $\beta_j(\mathbf{x})a_j(\mathbf{x})a_0^{-1}$  ;  
14    if  $\tau < \Delta t$  then  
15      Perform  $\tau$ -leaping up to  $t + \tau$  (w/ props.  $(1 - \beta_j(\mathbf{x}))a_j(\mathbf{x})$ ) ;  
16       $\mathbf{X}(t + \tau) = \mathbf{X}(t) + \boldsymbol{\nu}_j$  ;  
17       $t = t + \tau$  ;  
18    else  
19      Perform  $\tau$ -leaping up to  $t + \delta t$  (w/ props.  $(1 - \beta_j(\mathbf{x}))a_j(\mathbf{x})$ ) ;  
20       $t = t + \delta t$ .
```

Remark 3.3 *Choosing one blending function per reaction is a modeling choice that tries to fully exploit the multiscale nature (when present) of the chemical kinetics. A more conservative approach would be to define a single blending function for all reactions. As long as this choice of blending function sensibly partitions the state space, i.e. ensuring that the underlying stochastic process spends some time outside the SSA region, it would still lead to an algorithm that is more efficient than SSA.*

Remark 3.4 *The idea of partitioning the state space is rather general. In particular, one could replace τ -leap with the numerical method of their choice and the only thing that would need to be considered is how to do the simulation in the region of space where the numerical method co-exists with τ -leap. An example of this is the hybrid CLE method proposed in [29] where instead of using τ -leap one simulates the term $P_r \left(\int_0^t (1 - \beta_r(\mathbf{X}(s))) a_r(\mathbf{X}(s)) ds \right)$ in (6) by using the diffusion approximation.*

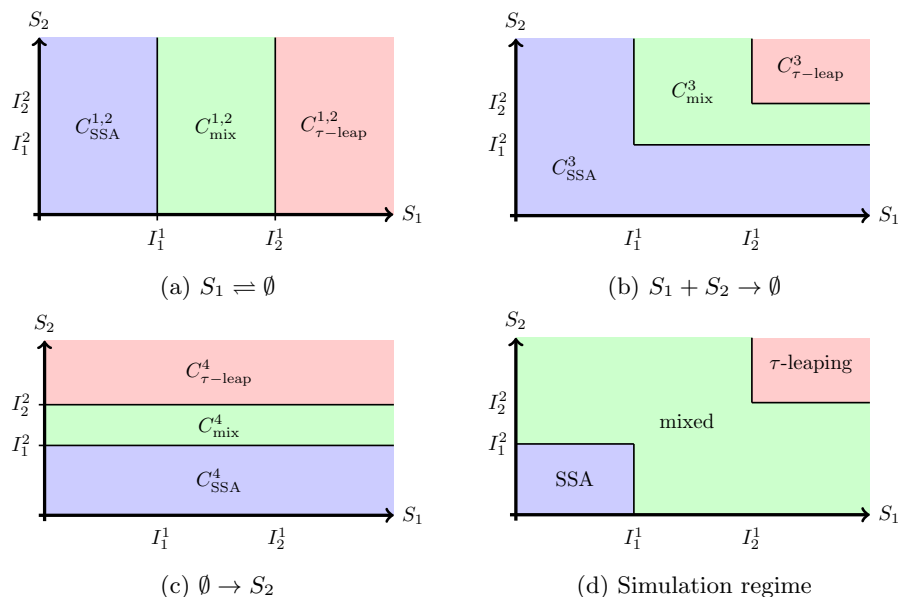


Figure 1: (a)-(c): Illustration of C_{SSA}^r , C_{mix}^r , $C_{\tau-leap}^r$ associated with each of the reactions of the chemical system in Example 3.1; (d): Partition of state space as per applicable simulation regime

4 Numerical Investigations

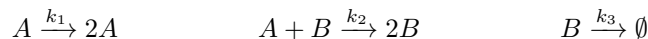
We now present several different numerical experiments to illustrate the robustness and the accuracy of our proposed approach. In particular, in Section 4.1 we study three different model chemical systems and compare the performance of hybrid τ with other algorithms. Furthermore, in Section 4.2 we study the performance of the hybrid- τ method when used as the stochastic simulator of choice for parameter estimation as described in Section 2.2.

4.1 Comparison with other numerical methods

4.1.1 Lotka-Volterra System

We begin by considering a stochastic version of the Lotka-Volterra system. It is a first example where the Hybrid- τ algorithm captures the correct statistical behaviour, while the standard CLE approximation (with reflective boundary conditions) completely fails to do so. The system is defined as:

Chemical System 1 *Lotka-Volterra System*



The molecules of A and B are in a predator-prey relationship, both populations oscillating between states of abundance and scarcity. As in [29], the reaction

constants are set to $k_1 = 2$, $k_2 = 0.002$, $k_3 = 2$. In Figure 2, a histogram is generated using 10^3 SSA realisations simulated until $T = 5$, which corresponds to one period of the solution to the corresponding Reaction Rate Equations. The initial conditions are chosen to be $A(0) = 50, B(0) = 60$. The system clearly exhibits a multiscale behaviour, spending time in all possible configurations of scarcity and abundance for both species. The locally high copy numbers of species cause the simulation via SSA to become excessively slow, and calls for employing approximate but accelerated schemes. The CLE is a standard choice; the CLE associated to the chemical system 1 is given by

$$\begin{aligned} dA(t) &= \left(k_1 A(t) - k_2 A(t) B(t) \right) dt + \sqrt{k_1 A(t)} dW_1(t) - \sqrt{k_2 A(t) B(t)} dW_2(t) \\ dB(t) &= \left(k_2 A(t) B(t) - k_3 B(t) \right) dt + \sqrt{k_2 A(t) B(t)} dW_2(t) - \sqrt{k_3 B(t)} dW_3(t). \end{aligned}$$

As previously discussed, the numerical simulation of this equation is problematic because of issues of non-negativity. To ensure the positivity of the system, we thus simulate the CLE using reflective boundary conditions.

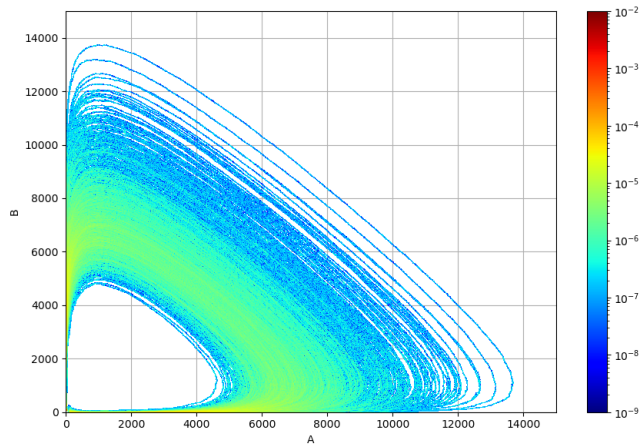


Figure 2: Histogram of 10^3 SSA simulations up to time $T = 5$ of the Lotka-Volterra system with $A(0) = 50, B(0) = 60$.

Figure 3 displays the numerical means of A computed using respectively SSA, the Hybrid τ , the Hybrid CLE [29] and the CLE (with reflective boundary conditions) with 10^4 samples. For the hybrid algorithms, the parameters are set to $(I_1^i, I_2^i) = (5, 10)$ and the step sizes $\Delta t = 10^{-2}$ and $\delta t = 10^{-3}$. The step-sizes were chosen manually by computing the error for a number of short exploratory runs. A more sophisticated implementation of the hybrid τ algorithm would require an adaptive scheme for the τ -leap part of the process. As we can observe, the numerical means of hybrid τ and hybrid CLE follow the same trend as SSA, whereas the CLE simulation completely fails to capture the right behaviour.

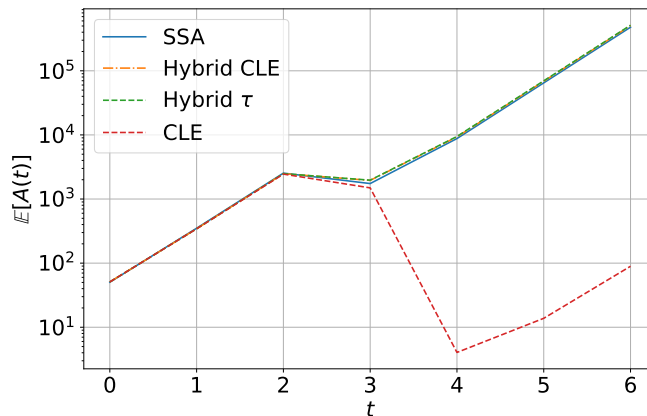


Figure 3: Numerical means of $A(t)$ using SSA, hybrid CLE, hybrid τ , and CLE with reflective BC

4.1.2 Schlögl System

We now study the Schlögl system taken from [45]. It is a non-linear model where the density function of the main reactant S displays bistability for a certain choice of reaction constants.

Chemical System 2 *Schlögl System*



where B_1 and B_2 are buffered species, i.e. their populations are kept at constant values $N_1 = 10^5$ and $N_2 = 2 \cdot 10^5$ respectively. In effect, only S needs to be tracked and this results in the following propensity functions:

$$a_1(x) = \frac{c_1}{2} N_1 x, \quad a_2(x) = \frac{c_2}{6} x(x-1)(x-2), \quad a_3(x) = c_3 N_2, \quad a_4(x) = c_4 x.$$

We set $c_1 = 3 \cdot 10^{-7}$, $c_2 = 10^{-4}$, $c_3 = 10^{-3}$ and $c_4 = 3.5$. In Figure 4a we plot one trajectory of the system for this choice of parameters for time $T = 10^6$ using the SSA. As we can see the system exhibits a bistable behaviour as it tends to spend time around two peaks one located around 80 and one around 560.

We experimented similarly to what was done in [45], comparing the numerical probability distributions obtained from the SSA and hybrid τ . For both algorithms, the following two blending regions were tested: (25, 35), (45, 55). Additionally, two pairs of time step sets (TSS) were tested, $(\Delta t, \delta t) = (10^{-2}, 10^{-3})$ and (0.25, 0.25). The initial condition is given by $S(0) = 250$. For each combination of parameters, 10^6 paths were generated up to time $T = 50$. Note that this time is not large enough so as for the system to jump between the two peaks

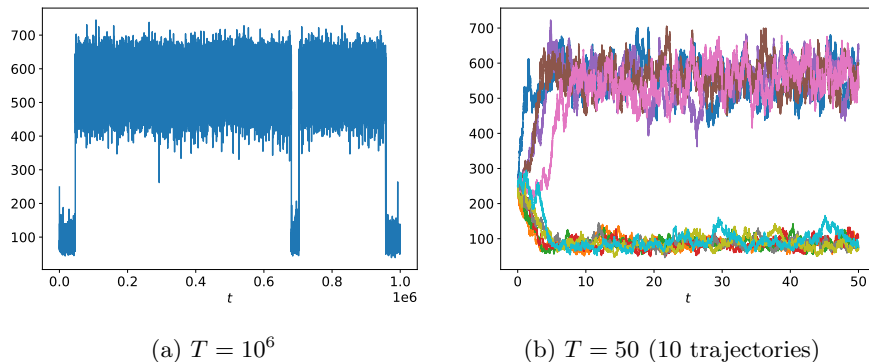


Figure 4: Trajectories of the Schlögl chemical system

			Timings [s]		Ratio SSA	
			low peak	high peak	low peak	high peak
Hybrid τ	TSS1	IS1	3.980222e-03	4.501482e-03	4.19	48.54
		IS2	4.191844e-03	4.741473e-03	3.98	46.08
	TSS2	IS1	1.997728e-04	1.884384e-04	83.45	1159.43
		IS2	1.959438e-04	1.863899e-04	85.08	1172.17
SSA		1.667085e-02	2.184813e-01	1	1	

Table 1: Time $\{s\}$ to simulate low and high trajectories of the Schlogl system, averaged over 500 simulations. Time Step Sets : TSS1 = $(10^{-2}, 10^{-3})$, TSS2 = $(0.25, 0.25)$; Interval Sets : IS1 = $(35, 45)$, IS2 = $(45, 55)$.

of distribution as we can see in Figure 4b in which we plot 10 trajectories of the system using SSA.

The results of our experimentation can be seen in Figure 5. As we can see for the same choice of TSS the position of the blending region hardly affects the approximation of the probability distribution $p(S(50)|S(0) = 250)$. Furthermore, when comparing with SSA there is hardly any difference between the numerical probability distribution for TSS1 and the true probability distribution as calculated by SSA. In contrast, for TSS2 the numerical bias is visible. As can be seen in Table 1 From a computational point of view, though both choices of the time-step lead to significant benefits since for TSS1 is roughly 4 times faster than SSA for the trajectories that get attracted towards the first peak and 50 times faster for the trajectories that get attracted towards the second peak. The corresponding ratios for TSS2 are and respectively indicating further computational benefits with the cost of increased bias.

4.1.3 Autorepressive System

Finally, we consider the autorepressive genetic system, taken from [46]. This is yet another example where chemical reactions happen on different scales. In this

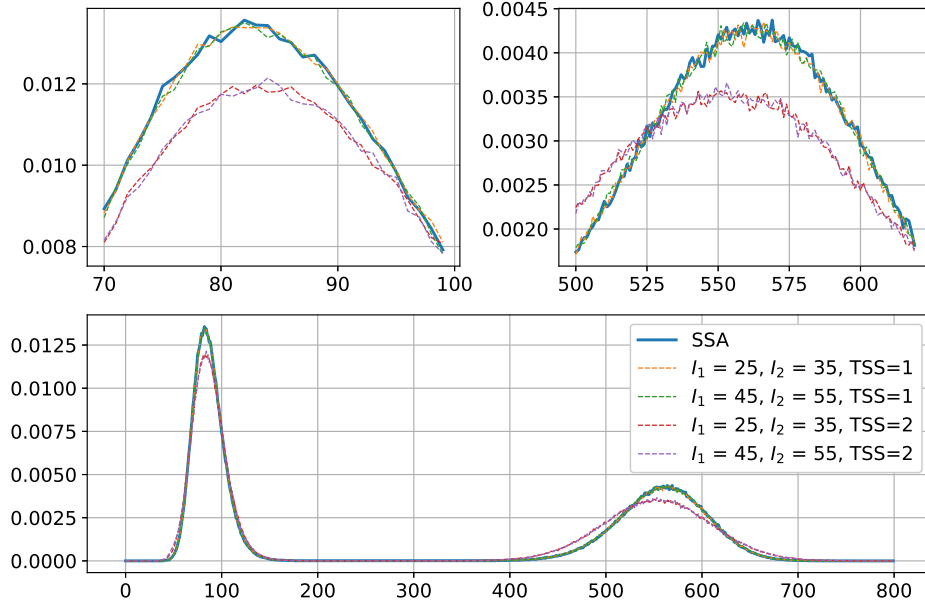
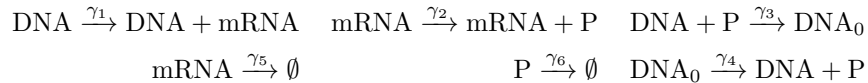


Figure 5: Schlögl system probability density function at $T = 50$ using Hybrid τ . Two time step sets (TSS) were used, $(10^{-2}, 10^{-3})$ and $(0.25, 0.25)$.

gene regulatory system, the DNA is only present in one or two copies (active or inactive), the messenger RNA (mRNA) and proteins may reach much higher numbers. The system is described as follows:

Chemical System 3 *Autorepressive Gene System*



In essence, the active DNA is transcribed to mRNA at rate γ_1 , which in turn produces proteins (P) at rate γ_2 . A protein may repress the active DNA, causing it to become inactive (represented by DNA_0) at rate γ_3 . The inactive DNA reactivates at rate γ_4 . Finally, the mRNA and the proteins are degraded at rates γ_5 and γ_6 respectively.

The reaction rates are set to $\gamma_1 = 10^{-2}$, $\gamma_2 = 0.5$, $\gamma_3 = 0.1$, $\gamma_4 = 10^{-2}$, $\gamma_5 = 5 \cdot 10^{-3}$ and $\gamma_6 = 0.2$. Both the Hybrid τ and the Hybrid CLE were used to simulate the system, and different blending regions were tested, $(5, 10)$, $(10, 15)$ and $(15, 20)$; the time steps were set to $\Delta t = 10^{-2}$ and $\delta t = 10^{-3}$. For each combination of parameters, 10^4 simulations were performed up to time $T = 10^3$. The means and variances of these different processes are detailed in Tables 2 and 3. The results again seem to indicate a certain robustness with respect to the chosen blending region.

Method	I_1	I_2	DNA	DNA ₀	Proteins	mRNA
SSA			0.1261	0.8739	63.278	25.279
Hybrid CLE	5	10	0.1257	0.8743	62.808	25.123
Hybrid CLE	10	15	0.1295	0.8705	62.88	25.141
Hybrid CLE	15	20	0.1269	0.8731	62.683	25.082
Hybrid τ	5	10	0.1311	0.8689	62.675	25.081
Hybrid τ	10	15	0.1277	0.8723	62.611	25.072
Hybrid τ	15	20	0.1279	0.8721	62.193	24.855

Table 2: Mean values of the Autorepressive Gene-regulatory System at $T = 10^3$ with sample size $N = 10^4$ using SSA, Hybrid CLE and Hybrid- τ algorithm with variable I_1, I_2 parameters.

Method	I_1	I_2	DNA	DNA ₀	Proteins	mRNA
SSA			0.33196	0.33196	33.424	13.046
Hybrid CLE	5	10	0.33151	0.33151	32.982	12.953
Hybrid CLE	10	15	0.33575	0.33575	32.846	12.857
Hybrid CLE	15	20	0.33286	0.33286	33.275	12.923
Hybrid τ	5	10	0.33751	0.33751	32.736	12.824
Hybrid τ	10	15	0.33376	0.33376	33.005	12.905
Hybrid τ	15	20	0.33398	0.33398	33.124	12.861

Table 3: Standard deviations of the autorepressive gene-regulatory system at $T = 10^3$ with sample size $N = 10^4$ using SSA, Hybrid CLE and Hybrid- τ algorithm with variable I_1, I_2 parameters.

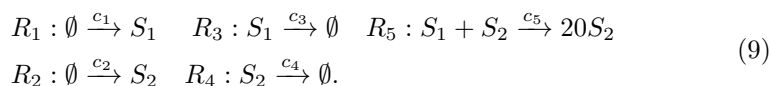
4.2 Parameter estimation

This section investigates the reliability of the Hybrid- τ algorithm for Bayesian inverse problems, in the setting described in Section 2.2

4.2.1 Experiment setting

The system on which the parameter estimation is performed is defined by the reactions (see also [16]):

Chemical System 4 *Bayesian inference system*



R_1 and R_2 are production reactions, R_3 and R_4 are decay reactions, and R_5 is a second-order reaction. The reaction rates are given by

$$\mathbf{c} = (2, sc, 1/50, 1, 1/(50 \cdot sc)),$$

where sc is used as a parameter, that takes the values $sc \in \{1, 10, 10^2, 10^3\}$. We aim to infer the value of \mathbf{c} for each of those values. To ensure identifiability, c_3 is set to its true value 1 in all simulations – hence practically, the Bayesian inference is performed on (c_1, c_2, c_4, c_5) .

Following [16], the noisy measurements are assumed to follow the distribution

$$\mathbf{Y}_i^n | \mathbf{X}_i(t_n) \sim \begin{cases} \text{Poisson}(\mathbf{X}_i(t_n)) & \text{if } \mathbf{Y}_i(t_n) > 0, \\ \text{Bernoulli}(0.1) & \text{else.} \end{cases} \tag{10}$$

4.2.2 Methodology

We are now interested in calculating the posterior distribution $p(\mathbf{c} | \mathbf{y}_{[0,T]})$. We do this using the Algorithms 2.4 and 2.5.

There are a number of modeling choices and parameter tuning that need to be done before we proceed with our numerical experiments and comparisons. In particular, in Algorithm 2.4 we use a Gaussian proposal kernel $q(\cdot | \mathbf{c})$ with mean \mathbf{c} and a covariance $\gamma \hat{\mathbf{C}}$ which will be estimated from exploratory runs with the objective to have acceptance probability of 10%. Overall using consecutive short exploratory runs of the particle filter with $\gamma = 1$, $\hat{\mathbf{C}} = I$ (Algorithm 2.4) allows us to successively determine a first estimate of the parameter by \mathbf{c}_{pre} and its covariance matrix $\hat{\mathbf{C}}$ (ii) the number of particles N , such that $\text{Var}(\log \hat{\mathbb{P}}(\mathbf{y} | \mathbf{c}_{pre}))$ does not exceed 2.5, and (iii) the scaling parameter γ , such that the accept-reject ratio is close to 10%. The choice of the number of particles N_{part} in step (ii) and the acceptance probability in step (iii) are the same as in [47].

After those values are determined, a small burn-in phase is performed to ensure the particle filter starts in a credible region. Finally, the actual experiment is run with $n_{iter} = 2 \cdot 10^5$ iterations, using the last explored state of the burn-in

	N_{part}		γ	
	SSA	Hybrid- τ	SSA	Hybrid- τ
$sc = 1$	800	320	0.05	2.0
$sc = 10$	640	1280	4.0	1.0
$sc = 10^2$	80	160	1.0	1.0
$sc = 10^3$	320	160	2.0	1.0

Table 4: Experimental values obtained for particle filter simulation.

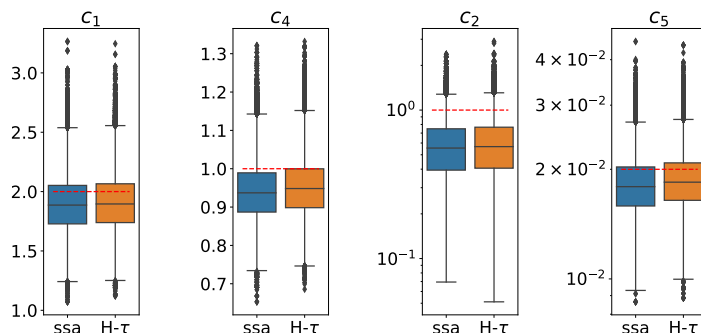


Figure 6: $sc = 1$.

phase as the starting point. This procedure is repeated for each value of sc , and for simulations obtained via the SSA or via the Hybrid τ . We summarise the obtained values in Table 4.

The values $(N_{\text{part}}, \gamma)$ chosen by in the setup phase bootstrap are roughly of the same order for both forward simulators. This suggests that the Hybrid- τ simulates the system in the same way as SSA, and thus causes the particle filter to explore the state space in the same way as (only much more efficiently when sc becomes large).

4.2.3 Numerical Results

We run the inference procedure using either the standard SSA or the Hybrid τ algorithm. As can be seen in the box-and-whiskers plots (Figures 6–7), across all scales the inference of the parameters c_1, c_2, c_4, c_5 are similar no matter which simulator is used. In all plots, the dashed red line represents the true value to be inferred. The colored boxes are delimited by the first and third quartiles, the whiskers have length $1.5 \times \text{IQR}$ (interquartile range), and the points outside are statistical outliers. The values c_1 and c_4 have no multiscale dependence, while the parameters c_2 and c_5 do.

The major difference is noted in the computational times, Figure 8 illustrates how, as the system becomes displays stronger multi-scale behaviour, the simulation time using the Hybrid- τ algorithm is bounded, while the SSA simulation

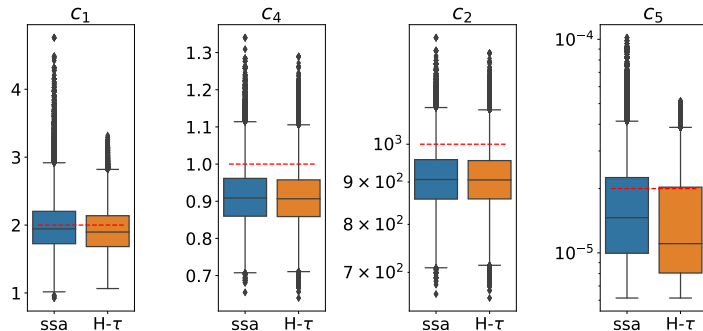


Figure 7: $sc = 10^3$

time grows linearly.

5 Conclusions

We have proposed a novel hybrid τ algorithm, inspired by the hybrid CLE method proposed in [29]. Unlike it, the quantities remain fully discrete at all times. The method leverages the splitting property of Poisson processes to rewrite the stochastic process as a sum of Poisson random variables that are simulated using SSA or τ -leaping; the computational gains become obvious when one manages to ensure that the reactions fired frequently are simulated using the τ -leaping, while those firing less often (and for which small stochastic variations may lead to important changes) are simulated using the exact SSA.

We point out that this algorithm really belongs to a larger class of hybrid schemes based on the splitting of the Poisson process into separate processes that are simulated differently. In this sense, there is a significant amount of flexibility in the simulation of (multi-scale) stochastic chemical kinetics. Straightforwardly, one could swap the τ -leaping by a more robust algorithm such as binomial τ -leaping, R -leaping, etc. Other approaches such as a separation into multiple levels (e.g. micro-meso-macro) with a suitable simulation at each level are also possible.

The choice of blending function discussed in this article is a “cautious” one, as it considers all the involved species in a given reaction (reactants and products). This can be understood as dynamically tagging a reaction to be simulated using the SSA if any species is low, τ -leaping if all are abundant or a combination of both in the intermediate regime. Including the reactants in the blending functions makes intuitive sense, among others it can make the algorithm particularly robust to the issue of negative species. However, if it is known *a priori* that certain products do not have a significant impact on system (no feedback loops, etc), not including them in the blending function may prove to be computationally interesting as it would naturally result in a larger state space in

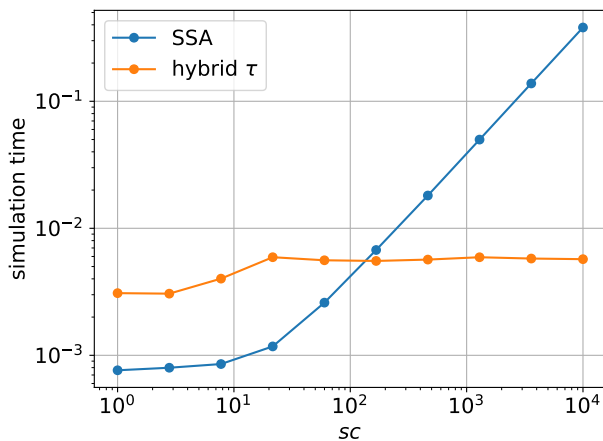


Figure 8: Mean simulation time for system (9) (averaged over 100 simulations) for different values of the parameter sc .

which the system is simulated with τ -leaping.

The various experiments presented in this article display how the hybrid τ algorithm produces accurate and computationally efficient results. This is especially the case in the multi-scale setting. The algorithm is naturally amenable to that setting, as it handles it with no necessary additional modelling steps, unlike other algorithms specifically designed for the multi-scale case such as e.g. Piecewise Deterministic Markov processes in [26]. The algorithm requires some user-prescribed values, the time-steps for the τ -leaping and for the intermediate regime, as well as the blending functions (additionally in our case, with their corresponding parameters I_1 and I_2). Numerically, it was observed that the dependence of the time-step sizes on the quality of the simulations is significantly more important than that of the blending regions. It would be of interest to investigate further the impact of the blending functions and regions, establishing criteria on how to suitably define them, as well as incorporating adaptive time-steps mechanisms for the different simulation regimes.

References

- [1] A. Arkin, J. Ross, and H. H. McAdams. Stochastic kinetic analysis of developmental pathway bifurcation in phage lambda-infected *Escherichia coli* cells. *Genetics*, 149(4):1633–1648, 1998.
- [2] J.M.G. Vilar, H.Y. Kueh, N. Barkai, and S. Leibler. Mechanisms of noise-resistance in genetic oscillators. *Proc. Natl. Acad. Sci.*, 99(9):5988–5992, 2002.

- [3] S. Kar, W. T. Baumann, M. R. Paul, and J. J. Tyson. Exploring the roles of noise in the eukaryotic cell cycle. *Proc. Natl. Acad. Sci.*, 106(16):6471–6476, 2009.
- [4] H. H. McAdams and A. Arkin. Stochastic mechanisms in gene expression. *Proc. Natl. Acad. Sci.*, 94(3):814–819, 1997.
- [5] P.S. Swain, M.B. Elowitz, and E.D. Siggia. Intrinsic and extrinsic contributions to stochasticity in gene expression. *Proc. Natl. Acad. Sci.*, 99(20):12795, 2002.
- [6] M. Doi. Stochastic theory of diffusion-controlled reaction. *J. Phys. A.-Math. Gen.*, 9(9):1479, 1976.
- [7] R. Erban and S.J. Chapman. Stochastic modelling of reaction–diffusion processes: algorithms for bimolecular reactions. *Phys. Biol.*, 6(4):1–18, 2009.
- [8] D. J. Higham. Modeling and simulating chemical reactions. *SIAM Review*, 50(2):347–368, 2008.
- [9] T. Jahnke and W. Huisinga. Solving the chemical master equation for monomolecular reaction systems analytically. *J. Math. Biol.*, 54(1):1–26, Jan 2007.
- [10] V. Wolf, R. Goel, M. Mateescu, and T. A. Henzinger. Solving the chemical master equation using sliding windows. *BMC Syst. Biol.*, 4(1):42, 2010.
- [11] S. MacNamara and K. Burrage. Krylov and steady-state techniques for the solution of the chemical master equation for the mitogen-activated protein kinase cascade. *Numer. Algorithms*, 51(3):281–307, 2009.
- [12] D. Schnoerr, B. Cseke, R. Grima, and G. Sanguinetti. Efficient low-order approximation of first-passage time distributions. *Phys. Rev. Lett.*, 119:210601, 2017.
- [13] D.T. Gillespie. Exact stochastic simulation of coupled chemical reactions. *J. Phys. Chem.*, 81(25):2340–2361, 1977.
- [14] M. A. Gibson and J. Bruck. Efficient exact stochastic simulation of chemical systems with many species and many channels. *J. Phys. Chem. A*, 104(9):1876–1889, 2000.
- [15] Y. Cao, H. Li, and L. Petzold. Efficient formulation of the stochastic simulation algorithm for chemically reacting systems. *J. Chem. Phys.*, 121(9):4059–4067, 2004.
- [16] C. Sherlock, A. Golightly, and C. S. Gillespie. Bayesian inference for hybrid discrete-continuous stochastic kinetic models. *Inverse Probl.*, 30(11):114005, 2014.

- [17] G. W. Molyneux and A. Abate. ABC(SMC)²: Simultaneous Inference and Model Checking of Chemical Reaction Networks. In A. Abate, T. Petrov, and V. Wolf, editors, *Computational Methods in Systems Biology*, pages 255–279, 2020.
- [18] D.T. Gillespie. Approximate accelerated stochastic simulation of chemically reacting systems. *J. Chem. Phys.*, 115(4):1716–1733, 2001.
- [19] A. Auger, P. Chatelain, and P. Koumoutsakos. R-leaping: Accelerating the stochastic simulation algorithm by reaction leaps. *J. Chem. Phys.*, 125:084103, 2006.
- [20] T. Tian and K. Burrage. Binomial leap methods for simulating stochastic chemical kinetics. *J. Chem. Phys.*, 121(21):10356–10364, 11 2004.
- [21] K. Burrage and T. Tian. Poisson runge-kutta methods for chemical reaction systems. *Advances in Scientific Computing and Applications*, 01 2004.
- [22] C. A. Yates and K. Burrage. Look before you leap: A confidence-based method for selecting species criticality while avoiding negative populations in tau-leaping. *J. Chem. Phys.*, 134(8):084109, 02 2011.
- [23] D. T. Gillespie. The chemical Langevin equation. *J. Chem. Phys.*, 113(1):297–306, 2000.
- [24] B. Hepp, A. Gupta, and M. Khammash. Adaptive hybrid simulations for multiscale stochastic reaction networks. *J. Chem. Phys.*, 142(3):034118, 2015.
- [25] C. Safta, K. Sargsyan, B. Debusschere, and H. N. Najm. Hybrid discrete/continuum algorithms for stochastic reaction networks. *J. Comput. Phys.*, 281:177–198, 2015.
- [26] S. Winkelmann and C. Schütte. Hybrid models for chemical reaction networks: Multiscale theory and application to gene regulatory systems. *J. Chem. Phys.*, 147(11):114115, 2017.
- [27] E. L. Haseltine and J. B. Rawlings. Approximate simulation of coupled fast and slow reactions for stochastic chemical kinetics. *Journal of Chemical Physics*, 117(15):6959–6969, 2002. Cited By :409.
- [28] A. Crudu, A. Debussche, and O. Radulescu. Hybrid stochastic simplifications for multiscale gene networks. *BMC Syst. Biol.*, 3(1):89, Sep 2009.
- [29] A. Duncan, R. Erban, and K. C. Zygalakis. Hybrid framework for the simulation of stochastic chemical kinetics. *J. Comput. Phys.*, 326:398–419, 2016.
- [30] D. T. Gillespie. A rigorous derivation of the chemical master equation. *Physica A Stat. Mech. Appl.*, 188(1):404–425, 1992.

- [31] D. F. Anderson and T. G. Kurtz. *Continuous Time Markov Chain Models for Chemical Reaction Networks*, pages 3–42. Springer New York, New York, NY, 2011.
- [32] D. T. Gillespie. Exact stochastic simulation of coupled chemical reactions. *J. Phys. Chem.*, 81(25):2340–2361, Dec 1977.
- [33] M.A. Gibson and J. Bruck. Efficient exact stochastic simulation of chemical systems with many species and many channels. *J. Phys. Chem. A.*, 104(9):1876–1889, 2000.
- [34] Y. Cao, D. T. Gillespie, and L. R. Petzold. Efficient step size selection for the tau-leaping simulation method. *J. Chem. Phys.*, 124(4):044109, 2006.
- [35] D. F. Anderson and M. Koyama. Weak error analysis of numerical methods for stochastic models of population processes. *Multiscale Model. Simul.*, 10(4):1493–1524, 2012.
- [36] Y. Cao, D.T. Gillespie, and L.R. Petzold. Avoiding negative populations in explicit Poisson tau-leaping. *J. Chem. Phys.*, 123(5):054104, 2005.
- [37] T.G. Kurtz. The relationship between stochastic and deterministic models for chemical reactions. *J. Chem. Phys.*, 57(7):2976–2978, 1972.
- [38] D. Schnoerr, G. Sanguinetti, and R. Grima. The complex chemical Langevin equation. *J. Chem. Phys.*, 141(2):024103, 07 2014.
- [39] D. F. Anderson, D. J. Higham, S. C. Leite, and R. J. Williams. On constrained langevin equations and (bio)chemical reaction networks. *Multiscale Model. Simul.*, 17(1):1–30, 2019.
- [40] C. Andrieu, A. Doucet, and R. Holenstein. Particle markov chain monte carlo for efficient numerical simulation. In P. L’ Ecuyer and A. B. Owen, editors, *Monte Carlo and Quasi-Monte Carlo Methods 2008*, pages 45–60, 2009.
- [41] C. Andrieu, A. Doucet, and R. Holenstein. Particle markov chain monte carlo methods. *J R Stat Soc Series B Stat Methodol.*, 72(3):269–342, 2010.
- [42] C. Andrieu and G. O. Roberts. The pseudo-marginal approach for efficient Monte Carlo computations. *Ann. Stat.*, 37(2):697 – 725, 2009.
- [43] N.J. Gordon, D.J. Salmond, and A.F.M. Smith. Novel approach to nonlinear/non-Gaussian Bayesian state estimation. *IEE Proc-F*, 140(2):107, 1993.
- [44] A. Doucet, S. Godsill, and C. Andrieu. On sequential Monte Carlo sampling methods for Bayesian filtering. *Statist. Comput.*, 10(3):197–208, 2000.

- [45] A. Abdulle, L. Gander, and G. R. de Souza. Optimal explicit stabilized postprocessed τ -leap method for the simulation of chemical kinetics. *J. Comput. Phys.*, 493:112482, 2023.
- [46] S. Winkelmann and C. Schütte. Hybrid models for chemical reaction networks: Multiscale theory and application to gene regulatory systems. *J. Chem. Phys.*, 147(11):114115, 2017.
- [47] C. Sherlock, A. H. Thiery, G. O. Roberts, and J. S. Rosenthal. On the efficiency of pseudo-marginal random walk Metropolis algorithms. *Ann. Stat.*, 43(1), February 2015.